RSC Advances

This article can be cited before page numbers have been issued, to do this please use: S. Gou, S. Luo, T. Liu, H. Xia, D. Jing, Q. Zhang, S. Li, Z. Li and Q. Guo, *RSC Adv.*, 2015, DOI: 10.1039/C5RA15434K.

ROYAL SOCIETY OF CHEMISTRY

www.rsc.org/advances

View Article Online
DOI: 10.1039/C5RA15434K

Graphical abstract

Thermally stable imidazoline-based sulfonate polymers for enhanced oil recovery

Shaohua Gou, Shan Luo, Tongyi Liu, Hong Xia, Dong Jing, Qin Zhang, Shiwei Li, Zhonghui Li and Qipeng Guo

Novel water-soluble imidazoline-based sulfonate copolymers were synthesized; the copolymers possess excellent thermal stability and outstanding potential for application in high-temperature oil recovery.

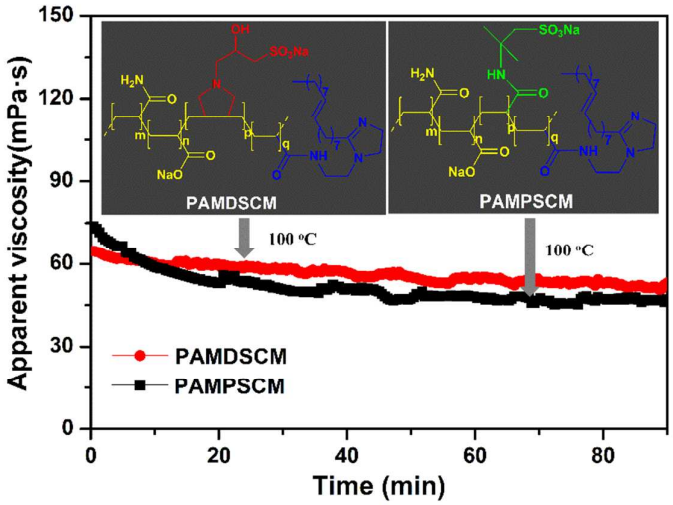

ROYAL SOCIETY OF CHEMISTRY View Article Online
DOI: 10.1039/C5RA15434K

RSC advances

ARTICLE

Thermally stable imidazoline-based sulfonate copolymers for enhanced oil recovery

naReceived 00th January 20xx,
Accepted 00th January 20xx

DOI: 10.1039/x0xx00000x

www.rsc.org/

Shaohua Gou, *[ab] Shan Luo,[b] Tongyi Liu,[b] Hong Xia,[b] Dong Jing,[b] Qin Zhang,[b] Shiwei Li,[b] Zhonghui Li [c] and Qipeng Guo*[d]

Novel imidazoline-based sulfonate copolymers (noted PAMDSCM and PAMPSCM) were successfully prepared by copolymerization of acrylamide (AM), acrylic acid (AA), 1-acrylamido ethyl-2-oleic imidazoline (ACEIM) with the sodium salts of 3-(diallyl-amino)-2-hydroxypropyl (NDS) or 2-acrylamido-2-methylpropane sulfonic acid (AMPS), respectively. The copolymers were characterized by infrared (IR) spectroscopy, ^{1}H nuclear magnetic resonance (^{1}H NMR) spectroscopy, pyrene fluorescence probe spectroscopy, viscosimetry and thermogravimetry (TG). Both PAMDSCM and PAMPSCM copolymers had excellent high-temperature tolerance in comparison with the same concentration of HPAM, and the residual viscosities were 32.0 mPa·s and 31.3 mPa·s (viscosity retention rates were 38.8% and 37.1%) at 140 °C, respectively. The copolymers possessed superior long-term thermal stability and their residual viscosity rates were up to 81.8% and 63.8% (52.9 mPa·s and 47.1 mPa·s) lasted 1.5 hours at 100 °C and 170 s^{-1}, respectively.

1.Introduction

Water-soluble polymers have been extensively used to maximize the residual oil in commercial chemical EOR applications.[1, 2] Hydrophobically associating polymer (HAPAM) thereof contains a small number of hydrophobic moieties attached directly to the polyacrylamide (PAM) backbone.[3-5] Those polymers, in comparison with partially hydrolyzed polyacrylamide (HPAM), have been proved to be effective in combating high salinity and relieving the downtrend of viscosity at high-temperature, which caused by the association of hydrophobic groups to minimize their exposure to the solvent.[6] Meanwhile, given its unique rheological properties, hydrophobically associating polymers possess excellent potential in EOR applications which was extensively reviewed in the work of Taylor in 1998.[7]

Numerous research efforts have focused on the introduction of special functional groups that benefit the improvement of water-solubility, temperature resistance, anti-shear property, salt tolerance and etc.[8-10] Sulfonate groups attached into the PAM chain can improve effectively the performance on confronting harsh environment like high temperature or high salinity.[11, 12] 2-Acrylamido-2-methylpropane sulfonic acid (AMPS), a widely used monomer, can be copolymerized with acrylamide (AM) to obtain a water-soluble sulfonate polymer that effectively improve thermal stability and salt tolerance.[13, 14] However, a safe temperature limit for AM-AMPS copolymer is recommended below 90 °C based on the investigations by Kamal et al.[15] In our previous studies, sulfonated copolymers have been proven to be successfully applied in EOR applications and possessed high performance on thickening property, temperature tolerance and salt resistance.[16-20]

Recently, increasing attention has been paid to multifunctional polymers, especially imidazole- and imidazoline-containing polymers which show a wide range of potential applications.[21-26] And the chemical architecture of substituted imidazoline units constituted as the following: a five-membered aromatic heterocyclic containing two nitrogen atoms at the 1, 3-positions (namely, an electron-rich hydrophilic amidine (N=C-N) motif), a hydrophobic alkyl chain and a pendant side chain constituted by electron-donor hydrophilic functional group(s) attached to N of the motif and the C terminal, respectively.[27] Although the particular configuration and characteristic endow imidazoline derivatives with desirable storage stability, viscosity, dispersibility and corrosion inhibition performance in various industrial applications, they were rarely utilized to incorporate into PAM chain for enhanced oil recovery.[28-33]

Here we report the synthesis and evaluation of imidazoline-based sulfonate copolymers (denoted as PAMDSCM and PAMPSCM) with the functional monomers attached to heterocyclic moieties and hydrophobic groups via free-radical copolymerization. The copolymers were characterized by IR, ^{1}H NMR, TG, and viscosimetry, respectively. The critical association concentrations of the polymer solutions were measured by the use of pyrene fluorescence probe. The corresponding polymers have been further examined on their unique properties, such as thickening ability, thermal stability, and shear thinning and salt tolerance.

2.Experimental

2.1 Materials

Acrylamide (AM), acrylic acid (AA), ammonium persulfate ($(NH_4)_2S_2O_8$), sodium bisulfite ($NaHSO_3$), 2-acrylamido-2-

View Article Online
DOI: 10.1039/C5RA15474K

methylpropane sulfonic acid (AMPS), ethanol, sodium hydroxide (NaOH), thionyl chloride, oleic acid, diethylenetriamine, xylene, epichlorohydrin, and diallyl amine are analytical reagent and used directly without further purification. The chemicals were gained from Chengdu Kelong Chemical Reagent Factory, therein partially hydrolyzed polyacrylamide (HPAM, 10% degree of hydrolysis, M_w=1.2×10^7), was obtained from Sichuan Guangya Polymer Chemical Co., Ltd.

2.2 Synthesis

2.2.1 Synthesis of ACEIM. Monomer 1-acrylamido ethyl-2-oleic imidazoline (ACEIM) was prepared referring to previously reported methods.[28, 34, 35] Briefly, an intermediate imidazoline derivative (aminoethyl oleic imidazoline) was synthesized based on oleic acid/diethylenetriamine in the ratio of 1:1.2 with xylene carrying generated water at 200-220 °C. Then extracted and further purified with ethyl acetate and deionized water after adding excessive NaCl saturated solution. Acryloyl chloride (2.172g, 0.024 mol) was slowly added dropwise to the intermediate product (6.99 g, 0.02 mol) which dissolved in 20 mL ethanol solution. The reaction was kept a temperature range of 0-10 °C for 4-5 h, and then the mixture was extracted with dichloromethane after the organic phase was washed three times with saturated NaCl solution. Finally, brown oil-soluble thick liquid, 1-acrylamido ethyl-2-oleic imidazoline (ACEIM) was further purified by the reduced pressure distillation of the third filtrate. The structure of ACEIM is shown in Fig.1. ACEIM: ^{1}H NMR (400 MHz, $CDCl_3$, Fig.3(a)): δ=7.29 (k, H, CH_2=C***H***CO–), 6.25-6.28 (k, 2H, C***H***$_2$=CHCO–), 5.92 (h, 2H, (CH_2)NC***H***$_2$CH$_2$N=), 5.33 (f, 2H, –$(CH_2)_7$C***H***=C***H***$(CH_2)_7CH_3$), 4.05-4.07 (g, 2H, =NC***H***$_2$CH$_2$N–), 3.38-3.51 (e, 2H, –NHCH$_2$C***H***$_2$NCO), 2.75 (d, 2H, –CONHCH$_2$C***H***$_2$N–), 1.99-2.22 (c, 14H, –(C***H***$_2)_7$CH=CH$(CH_2)_7CH_3$), 1.25 (b, 14H, –$(CH_2)_7$CH=CH(C***H***$_2)_7CH_3$), 0.87 (a, 3H, –C***H***$_3$), ppm.

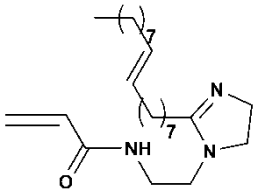

ACEIM

Fig.1 The structure of ACEIM.

2.2.2 Synthesis of Copolymers PAMDSCM and PAMPSCM. Copolymers PAMDSCM and PAMPSCM were conducted to prepare by acrylamide (AM), acrylic acid (AA), 1-acrylamido ethyl-2-oleic imidazoline (ACEIM), and 3-(diallyl-amino)-2-hydroxypropyl (NDS)/2-acrylamido-2-methylpropane sulfonic acid (AMPS) via free radical copolymerization in aqueous solution, respectively, and their synthesis routes are shown in Scheme 1. The optimal copolymerization conditions are recorded in Table 1. The copolymerization conditions (Fig.S1) and synthesis routes of the monomers (Scheme S1) are given in ESI†.

2.3 Characterization

2.3.1 IR. The copolymers were individually characterized by using WQF-520 Infrared spectroscopy (Beijing Rayleigh Analytical Instrument (Group) Co.Ltd, China) in 4400-400 cm^{-1} optical range.

2.3.2 ^{1}H NMR. The ^{1}H NMR spectra analyses of the polymers (dissolved in deuterium oxide (D_2O) solvent) were measured by a Bruker AV III-400 MHz spectrometer (Bruker BioSpin, Switzerland).

2.3.3 Intrinsic viscosity [η] measurement. The intrinsic viscosity of polymer solutions was gauged via an Ubbelohde viscometer. The copolymers were dissolved and diluted to the required concentration by way of the 1.0 mol/L NaCl solution at a constant temperature bath (30 °C). The flux time of polymer solutions were fain registered with an accuracy of 0.05 s.

2.3.4 Conversion measurement. The conversion of AM was performed with a high-performance liquid chromatography (HPLC; Shimadzu Co., Japan). The conversion was calculated by the residual AM of precipitated the polymer in ethanol, following equation 1: [36]

$$W(\%) = \frac{W_{AM} - \frac{AC_0}{A_0} \times V}{W_{AM}} \times 100\% \qquad (1)$$

here W(%) is the conversion of AM suggesting the conversion of copolymer; W_{AM} is the total weight of AM before reaction; A and A_0 are the chromatographic peak areas of the residual AM in ethanol and the standard sample AM, respectively; C_0 is the concentration of standard sample AM solution; V is the volume of ethanol solution precipitated by the polymer.

2.3.5 Pyrene fluorescence probe. Pyrene fluorescence probe was utilized to characterize the critical association concentration (CAC) of the copolymers by a Shimadzu RF-5301PC pectrofluoro-photometer with emission at 335 nm at 25 °C. The slit width of excitation (emission) was fixed at 15.0 nm through a constant scan speed of 800 nm/min and the spectral range was 350-580 nm. The corresponding polymers were diluted to different concentrations (100-4000 mg/L), whereby the concentration of pyrene was 2×10^{-6} mol/L.

2.4 TG test

The thermal stability of the polymers was conducted to measure by a thermogravimetric analyzer (Switzerland, METTLER TOLEDO Co.) for a flow rate of 20 mL/min at 25-800 °C. The heating rate of the TG experiments was 25 °C/min under nitrogen atmosphere.

2.5 Rheological characterization

2.5.1 Temperature resistance test. Temperature resistance tests of 2000 mg/L copolymer solutions were performed at a temperature range of 25-140 °C using a rotational rheometer (Haake RheoStress 6000, Germany) at 170 s^{-1}.

2.5.2 Long-term thermal stability test. Long-term thermal stability of 2000 mg/L copolymer solutions were achieved by deducing the relationship between apparent viscosity and time using a rotational rheometer (Haake RheoStress 6000, Germany) lasted 1.5 hours with a constant temperature of 100 °C at 170 s^{-1}.

2.5.3 Anti-shear test. Shear-tolerance of 2000 mg/L copolymer solutions were measured by a rotational rheometer (Haake RheoStress 6000, Germany) with a shear rate rang of 7.34-1000 s^{-1} at 25 °C.

2.5.4 Shear recovery test. Shear recovery performance of 2000 mg/L copolymer solutions were performed with stepped shear rate

(170 s^{-1}, 510 s^{-1} and 850 s^{-1}) at 25 °C by a rotational rheometer (Haake RheoStress 6000, Germany).

2.5.5 Viscoelasticity test. The viscoelastic characteristics of the copolymer (2000 mg/L) were investigated by a rotational rheometer (Haake RheoStress 6000, Germany) at 25 °C under a frequency (*f*) scanning range of 0.01-10 Hz, which obeyed Maxwell Model at lo shear frequency.

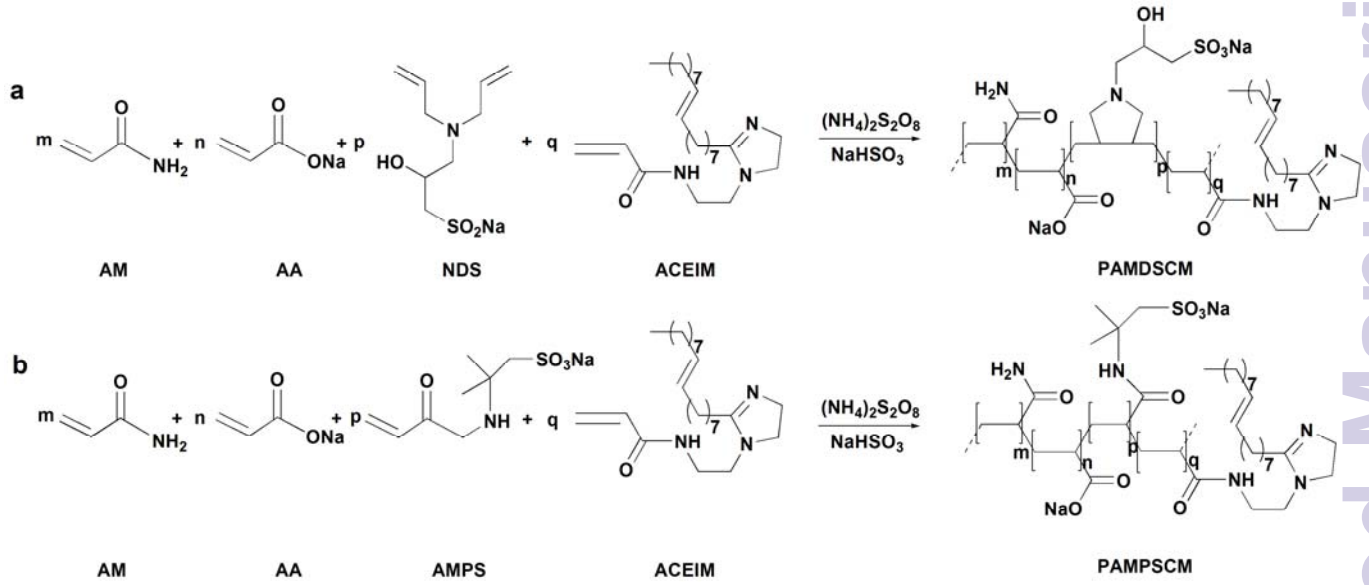

Scheme 1 Synthesis routes of PAMDSCM and PAMPSCM.

Table 1 Copolymerization conditions of PAMDSCM and PAMPSCM

Copolymer	Initiator (wt%)	pH	Temperature (°C)	Monomer (wt%)					Apparent viscosity (mPa·s)[a]	Intrinsic viscosity (mL/g)[b]	Conversion (%)[c]
				AM	AA	ACEIM	NDS	AMPS			
PAMDSCM	0.4	7	40	6.5	3.5	0.1	1.0	—	553.8	1178.2	95.9
PAMPSCM	0.4	7	40	7	3	0.15	—	1.0	571.1	1201.5	96.5

[a] 0.2 wt % polymer solution measured by a Brookfield DV-III+Pro viscometer at 25 °C

[b] The intrinsic viscosity was determined according to the reference[37]

[c] Conversion (wt%) of AM tested by HPLC

2.6 Salt resistance test.

Salt resistance tests of 2000 mg/L copolymer solutions were estimated by a Brookfield DV-III+Pro viscometer (Brookfield, USA) under different concentration inorganic salt (NaCl, $CaCl_2$ or $MgCl_2$) solutions at 25 °C. The composition of synthetic brine in the Long-term experiments is shown in Table 2.

Table 2 Composition of synthetic water flooding

ion	Na^+	K^+	Ca^{2+}	Mg^{2+}	Cl^-	HCO_3^-	SO_4^{2-}	Total
Concentration (mg/L)	2231	70	95	226	4026	28	549	7225

2.7 Core flooding test.

The effect of copolymer flooding on enhanced oil recovery was fulfilled under simulated high salinity at 85 °C. The dimension of sand-filled pipe prepared for the core experiments was about 2.5 cm in diameter and 50 cm in length. The total salinity of simulated brine across the core flooding experiments was about 7200 mg/L (see Table 2). The oil phase was prepared by simulated oil (67.4 mPa·s at 85 °C). The steel cylinders packed by silica sand were dried for a minimum of 24 hours before performing. The synthetic brine was initially infused the sand pack to the saturation, and subsequently injected the simulated crude oil. Then the sand pack was injected with the synthetic brine until the water content was above 95 %, and 2000 mg/L copolymer solution was followed to inject under a flow rate of 0.25 mL/min. The subsequent water flooding was eventually injected to replace polymer flooding until no more oil was exhausted. The oil recovery by polymer flooding (E_1) and the oil recovery by water flooding (E_2) were determined, respectively, thus the difference between them is the value of enhanced oil recovery (EOR).

3.Results and discussion

3.1 Characteristic analysis

3.1.1 IR analyses Described in Fig.2 are the IR spectra of the copolymers. The IR spectra presented that the monomer ACEIM was successfully copolymerized into the backbone of polymer chai based on characteristic peaks at 3429 cm^{-1}, 1653 cm^{-1}, 1561 cm^{-1}, 1458 cm^{-1}, 1404 cm^{-1}, and 1320 cm^{-1} in PAMPSCM IR spectrum and 3416 cm^{-1}, 1653 cm^{-1}, 1561 cm^{-1}, 1449 cm^{-1}, 1403 cm^{-1} and 1320 cm^{-1} in IR spectrum of PAMPSCM. As expected, the obvious absorption peaks occurred at 1117 cm^{-1} and 1043 cm^{-1} in PAMDSCM R

View Article Online
DOI: 10.1039/C5RA15434K

spectrum, and that of PAMPSCM IR spectrum was at 1108 cm^{-1} and 1043 cm^{-1}, implying the successful introduction of $–SO_3^-$ groups.

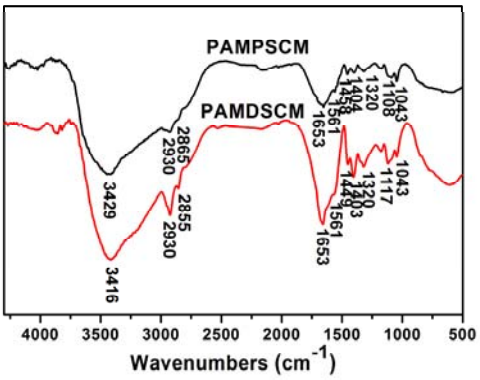

Fig.2 IR spectra of obtained copolymers.

3.1.2 ^{1}H NMR analyses. ^{1}H NMR spectra of PAMDSCM and PAMPSCM are shown in Fig.3. As displayed in Fig. 3(b), the chemical shift value was 7.67 ppm implying characteristic peak of the NH of [CON***H***CH_2–]. The chemical shift value appeared at 6.82 ppm due to the NH protons of [–CON***H***$_2$]. The chemical shift values were about 5.70 ppm and 5.53-5.56 ppm attributed to –NCH_2– of [(CH_2)N***C*****H**$_2$$CH_2$N=] and the aliphatic –CH=CH– of [–$CO(CH_2)_7$***C*****H**=***C*****H**$(CH_2)_7CH_3$], respectively, suggesting successful introduction of ACEIM. The peak value at 3.71 ppm was appointed to –CH_2N= proton of the imidazoline ring and the proton of–***C*****H**$_2$$SO_3$Na. The chemical shift value at 0.94 ppm was attributable to the –***C*****H**$_3$ protons of the aliphatic chain of monomer ACEIM. The protons of the aliphatic –CH_2– and polymeric chain were detected at 1.56-1.65 ppm. The chemical shift value of –CH– protons of polymeric chain was at 2.13 ppm. The peaks at 3.36-3.41 ppm represented the protons of [CONHC***H***$_2$$CH_2$–] and [–$CH_2$***C*****H**(OH)$CH_2SO_3$Na].

The ^{1}H NMR spectrum of copolymer PAMPSCM is depicted in Fig. 3(c), which was detected the similar morphological characteristic peaks with the polymer PAMDSCM. And the spectra peaks of copolymer PAMPSCM can be discovered the characteristic protons of the functional monomers. Those characteristic shift peaks, obviously, are indicative of the successful incorporation of the monomers ACEIM and AMPS. Depicted in ESI† is the ^{1}H NMR spectrum of monomer NDS (see Fig.S2).

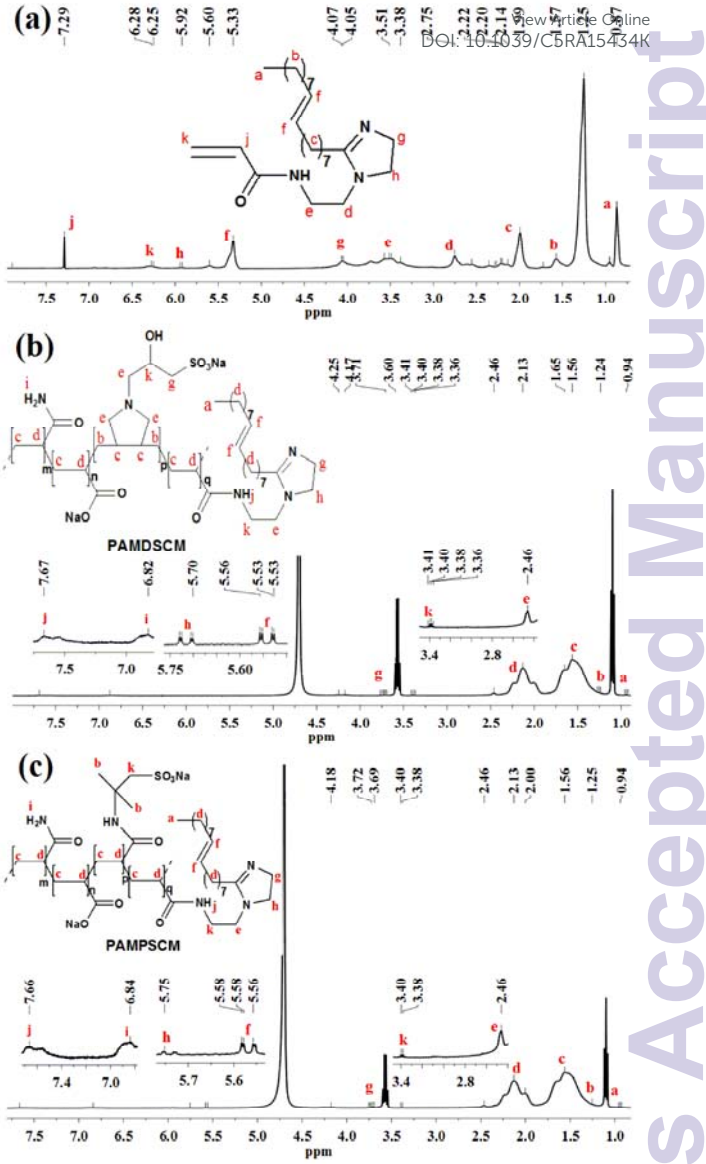

Fig. 3 ^{1}H NMR spectra of (a) ACEIM, (b) PAMDSCM and (c) PAMPSCM.

3.2 Critical association concentration

As a rule, the critical association concentration (cac) is well-defined as the concentration that the interchain associations start to decreases significantly with hydrophobic groups increasing.[38-40] The ratios of I_1 and I_3 as a function of different concentrations of the copolymers in fluorescence spectra (see Fig.S3 and Fig.S4, ESI†) were calculated, as displayed in Fig. 4(a). From the curves of I_1/I_3, a dramatic decrease was detected when the concentrations of polymer PAMPSCM exceeded 1.25 g/L, in which of polymer PAMDSCM occurred beyond 1.0 g/L. The decrease of I_1/I_3 values was associated with the weakening of the microenvironment polarity around pyrene molecule, suggesting that pyrene molecules transferred into the hydrophobic microdomains. And the results are also verified in the thickening curves of the polymers in Fig. 4(b).

Tackifying effect, one of the most considerable properties, was evaluated by measuring viscosity variation of the polymers solution at a concentration range of 100-4000 mg/L. As depicted in Fig. 4(b),

a linear increase on apparent viscosity was observed with the increasing of polymer concentration. Although the viscosity of HPAM solution started slightly higher than that of PAMDSCM and PAMPSCM at low concentration, the viscosities of PAMDSCM and PAMPSCM were well above that of HPAM when the concentration was above 600 mg/L. And from the viscosity curves, the breakthrough points of PAMDSCM and PAMPSCM were about 1.0 g/L and 1.25 g/L, respectively. It was due in part to the enhancement on association effect and hydrogen bond, suggesting the introduction of rigid imidazoline ring, hydrophobic groups and sulfonate groups.

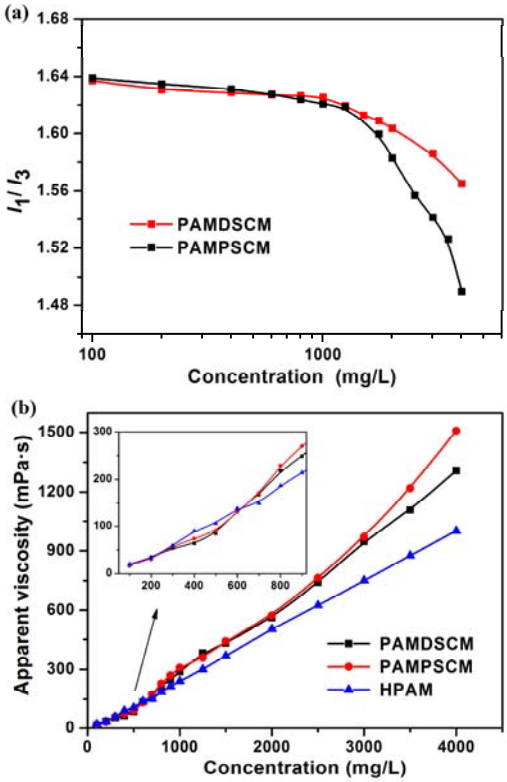

Fig. 4 (a) Effect of the copolymers on I_1/I_3 values; (b) the thickening properties of the copolymers.

3.3 TG analysis

The TG curves of PAMDSCM, PAMPSCM and HPAM are depicted in Fig.5. In the TG profiles, the mass loss declined consecutively over the whole temperature range of 25-800 °C. For PAMDSCM, the first weight loss was 12.7 wt% at 25-242 °C, showing the evaporation of crystal water existing in the polymers. The second steps appeared at 242-344 °C with a mass loss of 29.4 wt%, suggesting the thermolysis of the amide group, hydrophobic moiety, sulfonate group and imidazoline ring. The final mass loss beyond 344 °C was about 51.7 wt% corresponding to the decomposition of carbon backbone of the polymers. For PAMPSCM, the first one with a weight loss of 17.2 wt% occurred at 25-280 °C. The second stage took place at 280-583 °C with a mass loss of 44.9 wt%, which may be ascribed to the decomposition of the amide group, oleic imidazoline moiety and sulfonate group of the polymer. The final one occurred beyond 583 °C implying the carbonization. From the TG curves, hence, the mass loss of polymer PAMDSCM was lesser than that of PAMPSCM at 25-200 °C due in part to the additional five-membered ring structure formed by the diallyl. Moreover, a sharp weight decline of PAMDSCM was observed beyond 350 °C, which can be attributed to the hydroxy decomposition of monomer NDS. For HPAM, the first one took place at 25-211 °C with a mass loss of 16.3 wt%. The second stage with a weight mass of 35.8 wt% occurred at 211-374 °C caused by the decomposition of the amide groups. The last one occurred beyond 384 °C, suggesting the carbonization of HPAM.

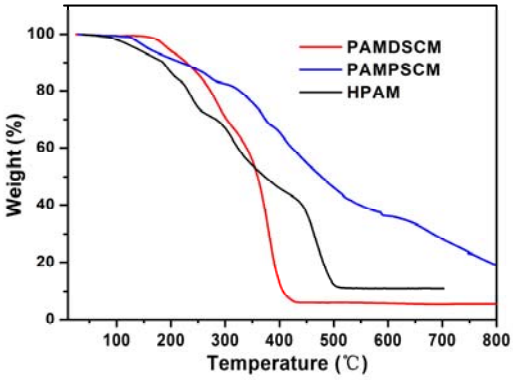

Fig. 5 Thermal gravimetric curves of the polymers.

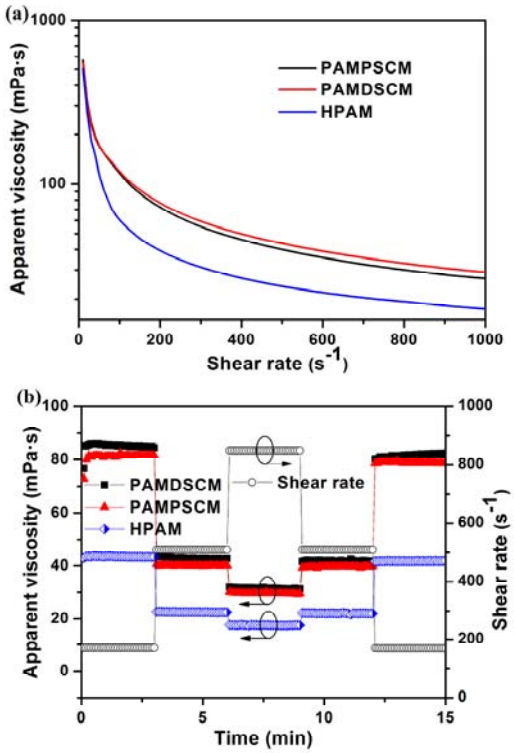

Fig. 6 (a) Anti-shear resistance and (b) shear recovery of the polymers.

3.4 Rheological behavior

3.4.1 Anti-shear resistance. Apparent viscosity dependent on shear rate for the copolymers are conducted to delineate in Fig. 6(a). Obviously, it was fantastically discovered the approximate decline curves of the polymers with the shear rate increasing. The viscosity of PAMDSCM or PAMPSCM fell abruptly at a shear rate range of 0.01-400 s^{-1} and maintained the continuous-steady viscosity over 400 s^{-1}. The viscosity/shear rate curves of copolymers PAMDSCM and PAMPSCM had superior anti-shear thinning and the polymer

possessed higher residual viscosities (29.1 mPa·s and 26.7 mPa·s, respectively), compared with the corresponding concentration HPAM solution (13.3 mPa·s) at 1000 s^{-1}. The results were indicated that the rigid structure of imidazoline monomer succeeded to induce an increase in viscosity retention rate and improved effectively anti-shear resistance of the polymers.

3.4.2 Shear recovery. The variations of apparent viscosity as a function of different gradient shear rates for PAMDSCM and PAMPSCM in aqueous phase are portrayed in Fig. 6(b). As expected, it was discovered that the viscosity curves of the polymer solutions kept approximate viscosity value, which undergone a flipping back and forth in the region of 170 s^{-1}, 510 s^{-1} and 850 s^{-1}, then back again. The phenomena indicated that the polymers functionalized imidazoline derivative possessed remarkable improvement on shear stability on a basis of the reversible supermolecular networks of hydrophobically associating polymer.[41]

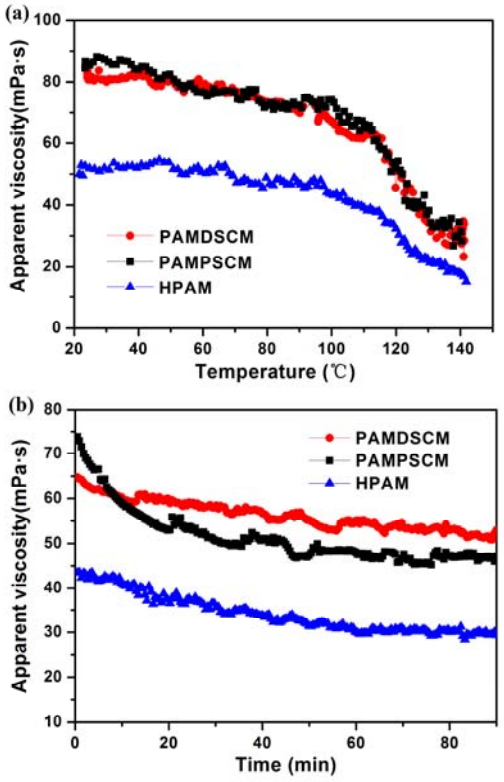

Fig. 7 (a) Effect of temperature on apparent viscosity; (b) the viscosity-time curves of the polymers at 100 °C.

3.4.3 Temperature tolerance. The variation of apparent viscosity as a function of different temperature for PAMDSCM and PAMPSCM in aqueous phase are depicted in Fig.7(a). At a temperature range of 25-110 °C, a continuously slow decrease in viscosity was initially observed in the approximate decline curves of PAMDSCM and PAMPSCM. As temperatures continue to rise, it was amazing that an abruptly decrease was subsequently observed. It could be derived that polymers PAMDSCM and PAMPSCM possessed the viscosity residual rate of 76% and 78% at 110 °C, respectively. And the residual viscosities were 32.0 mPa·s and 31.3 mPa·s, respectively, whereas that of HPAM was 17.5 mP·s at 140 °C. The phenomena can be interpreted in terms of the characteristic hydrophobic effect of hydrophobically associating polymers, suggesting that the successful introduction of ACEIM unit into PAM chain can effectively improve temperature tolerance on account of imidazoline ring within the rigid structure.

3.4.4 Long-term thermal stability. Long-term thermal stabilities of the polymers are depicted in Fig. 7(b). Obviously, it was discovered that those initially decreased slowly in viscosity, then kept approximately trend to be stable following the time increasing at 100 °C. As expected, the polymers possessed excellent long-term thermal stabilities in comparison to the same concentration HPAM, which depend on the physical reversibility of association effect of the polymers.[41, 42] What needs to be emphasized is that the viscosities of 2000mg/L of the polymers and HPAM solutions are virtually unanimous; however, the difference of the molecular weight between HPAM and obtained polymers is tremendous. And PAMDSCM held the preferable thermal stability than PAMPSCM solution through 90 min of 100 °C.

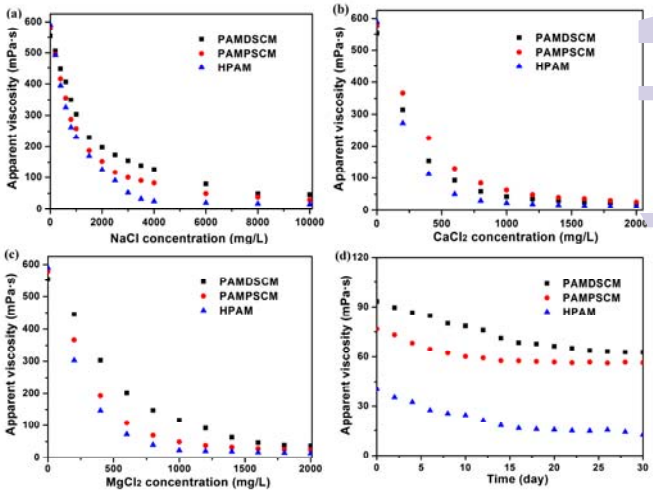

Fig.8 (a) Effect of NaCl concentration on apparent viscosity; (b) Effect of $CaCl_2$ concentration on apparent viscosity; (c) Effect of $MgCl_2$ concentration on apparent viscosity; (d) long-term stability of the polymers in the presence of 7225 mg/L inorganic salt for 30 days.

3.5 Salt resistance

The stabilities of the corresponding polymer solutions against inorganic salt (Na^+, Ca^{2+} or Mg^{2+}) are shown in Fig.8(a-c). For the curves of PAMDSCM and PAMPSCM, it was discovered that the apparent viscosity presented initially declined rapidly and subsequently plateaued with the addition of inorganic salt. It also can calculate that the residual viscosity were 46.2 mPa·s and 29.3 mPa·s for PAMDSCM and PAMPSCM in 10 000 mg/L NaCl solution, respectively, in which the residual viscosity of HPAM was 15.5 mPa·s. And the tests to resist Ca^{2+} (Mg^{2+}) for PAMDSCM and PAMPSCM are shown in Fig. 8 and the residual viscosity were 20.6 mPa·s and 25.7 mPa·s (37.1 mPa·s and 24.6 mPa·s, respectively) in 2000 mg/L inorganic salt, respectively. The polymers had preferable improvement on the salt resistance compared with HPAM solution (2000 mg/L $CaCl_2$: 11.6 mPa·s; 2000 mg/L $MgCl_2$: 13.6 mPa·s), which were associated with the enhancement of internal rotation resistance due to the introduction of hydrophobic group and sulfonate groups.

The variations of apparent viscosity of the polymers (2000 mg/L) in the presence of inorganic salt were determined by a Brookfield DV-III+Pro viscometer at 25 °C for 30 days, as shown in Fig.8(d). As observed in the curves, obviously, the viscosities of the polymers showed the similar decline tendency with time rising. The phenomena can be explained the electrostatic charge shielding effect in the presence of salt, hence a collapse of the network caused the reduction of the viscosity of the polymers.[43, 44] And obtained polymers can withstand preferably high salinity in comparison to the same concentration HPAM solution on account of the introduction of sulfonate and oleic imidazoline unit into the polymers chain.

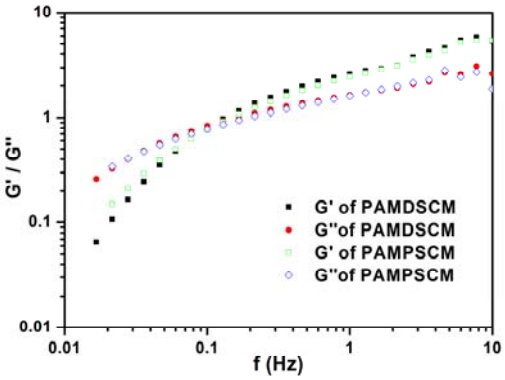

Fig.9 Viscoelasticity of the polymers.

3.6 Viscoelasticity

The viscoelastic properties of PAMDSCM and PAMPSCM solutions are depicted in Fig.9. As described in Fig.9, the dynamic viscoelastic curves of the storage modulus (*G′*) and loss modulus (*G″*) dependent on the oscillation frequency (*f*) presented approximate growth trend that *G′* and *G″* initially increased gradually (*G′*<*G″*) in the region of low-frequency, and subsequently *G′* surpassed *G″* that elastic behavior predominated accompanying with the frequency rising. Those are the characteristic viscoelastic behaviors of the imidazole-functional sulfonate polymers suggesting the great potential of enhanced recovery efficiency in EOR applications.

3.7 Enhanced oil recovery

The characteristic parameters for polymer solutions are investigated in Table 3 under simulated salinity environment in core flooding tests, which included resistance factor (*RF*), residual resistance factor (*RRF*), the recovery factor (E_1, E_2 and EOR value) and e... Obviously, it can be observed that the functionalized copolymers possessed superior profile control capability in a comparison with the same concentration of HPAM solution.

The results of oil recovery rate as a function of volume injected (PV) for PAMDSCM, PAMPSCM and HPAM solutions are plotted in Fig.10. The porosity and permeability across the core flooding tests were about 35.48% and 203.6 mD, respectively. Besides, the measurements of the porosity and permeability before and after the core flooding experiments showed that the difference was inconspicuous. From the curves, it was derived the oil recovery factor of PAMDSCM (EOR=12.3%) and PAMPSCM (EOR=10.25%), whereas that of HPAM was only 6.17 %. Given the unique steady and dynamic rheological properties of the polymers, relatively hi... oil recovery factors were obtained under simulated high temperature and salinities, thus the results were verified by the effective improvement of water-oil mobility ratio.

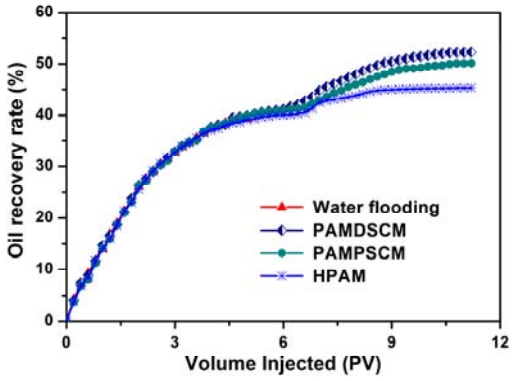

Fig. 10 The results of the core-flooding experiments.

Table 3 Characteristic parameters of polymer solutions

Core samples	Polymer solutions	*RF*	*RRF*	E_1 (%)	E_2 (%)	EOR (%)
1	PAMDSCM	12.53	4.02	52.19	39.89	12.30
2	PAMPSCM	13.05	4.60	50.12	39.87	10.25
3	HPAM	4.58	1.53	45.32	39.17	6.17

4.Conclusions

Novel imidazoline-functionalized sulfonate copolymers have been successfully synthesized in the presence of $(NH_4)_2S_2O_8$-$NaHSO_3$. The two copolymers possessed outstanding improvement on high thermal stability and their viscosity residual rates can be up to 38.8% and 37.1% at 140 °C in comparison with that of 25 °C, respectively. The polymers solutions also had excellent long-term heat stability that their residual viscosity rates could be up to 81.8% and 63.8% lasted 1.5 hours at 100 °C with a shear rate of 170 s^{-1}, respectively. Moreover, the copolymers have been confirmed to promote remarkably thickening and rheological property on a basis of the unique structural characteristic of hydrophobic copolymers. The copolymer solutions had been proven to be more effectively against the inorganic salt (NaCl, $CaCl_2$ or $MgCl_2$). Additionally, the EOR results inferred that PAMDSCM and PAMPSCM solutions could enhance the simulated oil recovery of 12.30% and 10.25%, respectively. The excellent features signified that the polymers hav... great technological potential in high-temperature oil recovery.

Acknowledgements

The work was financially supported by key projects (natural sciences) of Sichuan Provincial Education Department (15ZA0051), Foundation of Youth Science and Technology Innovation Team of Sichuan Province (2015TD0007) and Southwest Petroleum University (2014PYZ008, 2014XJZ759). The authors express their sincere thanks for the financial supporters.

Notes and references

1 Q. Chen, Y. Wang, Z. Lu and Y. Feng, *Polym. Bull.*, 2013, **70**, 391-401.
2 X. Liu, W. Jiang, S. Gou, Z. Ye, M. Feng, N. Lai and L. Liang, *Carbohyd. Polym.*, 2013, **96**, 47-56.
3 I. Iliopoulos, T. K. Wang and R. Audebert, *Langmuir*, 1991, **7**, 617-619.
4 S. Biggs, A. Hill, J. Selb and F. Candau, *J. Phys. Chemistry*, 1992, **96**, 1505-1511.
5 Y. Kakizawa, H. Sakai, K. Nishiyama, M. Abe, H. Shoji, Y. Kondo and N. Yoshino, *Langmuir*, 1996, **12**, 921-924.
6 K. C. Taylor and H. A. Nasr-El-Din, *Petroleum Society of Canada*, 2007.
7 K. C. Taylor and H. A. Nasr-El-Din, *J. Petrol. Sci. Eng.*, 1998, **19**, 265-280.
8 D. Wever, F. Picchioni and A. A. Broekhuis, *Prog. Polym. Sci.*, 2011, **36**, 1558-1628.
9 K. D. Branham, G. S. Shafer, C. E. Hoyle and C. L. McCormick, *Macromolecules*, 1995, **28**, 6175-6182.
10 V. A. Vasantha, S. Jana, A. Parthiban and J. G. Vancso, *Chem. Commun.*, 2014, **50**, 46-48.
11 A. Sabhapondit, A. Borthakur and I. Haque, *Energ. Fuel.*, 2003, **17**, 683-688.
12 M. Rashidi, A. M. Blokhus and A. Skauge, *J. Appl. Polym. Sci.*, 2011, **119**, 3623-3629.
13 M. Rashidi, A. M. Blokhus and A. Skauge, *J. Appl. Polym. Sci.*, 2010, **117**, 1551-1557.
14 W. O. Parker and A. Lezzi, *Polymer*, 1993, **34**, 4913-4918.
15 M. S. Kamal, A. S. Sultan, U. A. Al-Mubaiyedh and I. A. Hussein, *Polym. Rev.*, 2015, 1-40
16 Z. Ye, G. Gou, S. Gou, W. Jiang and T. Liu, *J. Appl. Polym. Sci.*, 2013, **128**, 2003-2011.
17 S. Gou, T. Yin, Z. Ye, W. Jiang, C. Yang, Y. Ma, M. Feng and Q. Xia, *J. Appl. Polym. Sci.*, 2014, **131**, DOI: 10.1002/app.41238.
18 S. Gou, T. Yin, L. Yan and Q. Guo, *Colloids. Surface. A.*, 2015, **471**, 45-53.
19 L. Yan, T. Yin, W. Yu, L. Shen, M. Lv and Z. Ye, *RSC Adv.*, 2015, **5**, 42843-42847.
20 S. Gou, Y. He, Y. Ma, S. Luo, Q. Zhang, D. Jing and Q. Guo, *RSC Adv.*, 2015, **5**, 51549-51558.
21 V. Bertini, M. Pocci, N. Picci and A. De Munno, *Eur. Polym. J.*, 1993, **29**, 871-875.
22 T. Seçkin, B. Alici, E. Çetinkaya and İ. Özdemir, *Polym. Bull.*, 1996, **37**, 443-450.
23 L. W. Chen and Y. H. Kuo, *Wiley Online Library*, 1997, **118(1)**. 117-127.
24 S. J. Welsch, M. Umkehrer, C. Kalinski, G. Ross, C. Burdack, J. Kolb, M. Wild, A. Ehrlich and L. A. Wessjohann, *Tetrahedron Lett.*, 2015, **56**, 1025-1029.
25 Y. Sano, M. Miyamoto, Y. Kimura and T. Saegusa, *Polym. Bull.*, 1982, **6**, 343-349
26 H. Tsutsumi, Y. Sumiyoshi, K. Onimura and T. Oishi, *Solid State Ionics*, 2003, **160**, 131-139
27 M. A. Mazumder, H. A. Al-Muallem and S. A. Ali, *Corros. Sci.*, 2015, **90**, 54-68.
28 S. Kamijo and Y. Yamamoto, *Chem-Asian. J.*, 2007, **2**, 568-578.
29 D. Bajpai and V. K. Tyagi, *J. oleo sci.*, 2006, **55**, 319-329.
30 P. McCormack, P. Jones and S. J. Rowland, *Rapid Commun. Mass Sp.*, 2002, **16**, 705-712.
31 D. Wang, S. Li, Y. Ying, M. Wang, H. Xiao and Z. Chen, *Corros Sci.*, 1999, **41**, 1911-1919.
32 K. Zhang, B. Xu, W. Yang, X. Yin, Y. Liu and Y. Chen, *Corros. Sci.*, 2015, **90**, 284-295.
33 M. A. Gough and G. J. Langley, *Rapid Commun. Mass Sp.*, 1999, **13**, 227-236.
34 M. A. Mazumder, H. A. Al-Muallem and S. A. Ali, *Corros. Sci.*, 2015, **90**, 54-68.
35 P. Gogoi and D. Konwar, *Tetrahedron Lett.*, 2006, **47**, 79-82.
36 S. Gou, M. Liu, Z. Ye, L. Zhou, W. Jiang, X. Cai and Y. He, *J. Appl. Polym. Sci.*, 2014, **131,** DOI: 10.1002/app.40166.
37 L. Alagha, S. Wang, Z. Xu and J. Masliyah, *J. Phys. Chem. C*, 2011, **115**, 15390-15402.
38 F. Giusti, J. Popot and C. Tribet, *Langmuir*, 2012, **28**, 10372-10380.
39 F. Petit-Agnely, I. Iliopoulos and R. Zana, *Langmuir*, 2000, **16**, 9921-9927.
40 J. Lin and S. Hou, *Macromolecules*, 2014, **47**, 6418-6429.
41 I. Nahringbauer, *Langmuir*, 1997, **13**, 2242-2249.
42 I. Nahringbauer, *J. Colloid Interf. Sci.*, 1995, **176**, 318-328.
43 X. Liu, W. Jiang, S. Gou, Z. Ye, M. Feng, N. Lai and L. Liang, *Carbohyd. Polym.*, 2013, **96**, 47-56.
44 J. Sukpisan, J. Kanatharana, A. Sirivat and S. Q. Wang, *J. Polym. Sci. Pol. Phys.*, 1998, **36**, 743-753.